Analysis of the maximum reinforcement loads of four MSE walls compared to the values predicted by the AASHTO 2020 specification

Keli Bohrer[1*], *and Delma* Vidal[2]

[1]PhD student, Technological Institute of Aeronautics, Department of Civil Engineering, 50 Pca Mal. Eduardo Gomes, Brazil
[2] Professor, Technological Institute of Aeronautics, Department of Civil Engineering, 50 Pca Mal. Eduardo Gomes, Brazil

Abstract. Mechanically stabilized earth (MSE) systems are a well-known and applicable solution for retaining walls, that presents a composite structure consisting of layers of backfill soil with rigid or flexible reinforcement inclusions. The stability of the wall system is derived from the interaction between the backfill and soil reinforcements involving friction and tension. The wall facing has as its main function to prevent erosion of the structural backfill. The design of MSE walls is usually divided in two phases: external and internal stability. Although there are many methods to design MSE walls, the Coherent Gravity Method is the most common used for MSE walls reinforced with inextensible (steel) reinforcements, the Simplified Method for both steel and geosynthetics reinforced wall systems and the new one included in 2020, Stiffness Method, to calculate the maximum reinforcement loads, T_{max}, for extensible (geosynthetics) reinforced MSE walls (all these methods are outlined in Section 11 of the AASHTO LRFD Bridge Design Specifications 2020) . The main objective of this paper is to carry out the analysis of the 3 methods available at AASHTO and compare the results from full-scale MSE walls and the predicted T_{max} values.

1 Introduction

Mechanically Stabilized Earth (MSE) retaining wall is a composite structure that incorporates layers of backfill soil with rigid or flexible reinforcement elements. The stability of this wall system relies on the interaction between the backfill and the soil reinforcements, which involves both friction and tension. The primary function of the wall facing is to prevent erosion of the structural backfill, resulting in a cohesive gravity structure capable of supporting substantial loads.

The properties and materials of the major components, including the backfill, reinforcement, and facing, can vary depending on the specific design criteria for the wall. Facing elements may take the form of modular precast concrete panels, precast blocks,

* Corresponding author: kelirbohrer@gmail.com

geosynthetic wrapping, or wire mesh. Soil reinforcements are typically composed of steel or geosynthetic materials in the form of strips or blankets. Each soil reinforcement option has its own characteristics related to pullout and tensile capacity, resistance to corrosion, and durability.

When it comes to the backfill material, several critical parameters should be analyzed, including gradation, plasticity, permeability, and strength. These parameters are essential for ensuring the overall stability and performance of the MSE retaining wall.

The design of MSE walls typically comprises two phases: external and internal stability. Different countries and states, often guided by their relevant expert institutions, establish their own specifications. These specifications are developed based on a combination of empirical data and analytical analysis to predict the behavior of MSE walls. In North America, notable specifications include those from AASHTO (American Association of State Highway and Transportation Officials), FHWA (Federal Highway Administration), CHBDC (Canadian Highway Bridge Design Code), NCMA (National Concrete Masonry Association), among others. These specifications are crucial for ensuring the stability and long-term performance of MSE walls.

While there are many specifications available, a significant portion of them is grounded in recommendations provided by AASHTO, making it a primary and widely recognized specification in North America for MSE wall design and construction.

In 2020, AASHTO introduced a new method for predicting the maximum reinforcement loads (T_{max}) in the design of MSE walls. When selecting the appropriate method for designing maximum load capacity in reinforcement, it is essential to understand the properties and behavior of the reinforcement material, which can vary between inextensible and extensible reinforcement types.

For MSE walls reinforced with inextensible reinforcement, typically steel, the Coherent Gravity Method is the most commonly employed approach. The Simplified Method is another option suitable for both steel and geosynthetic-reinforced wall systems.

However, for extensible reinforced MSE walls, those using geosynthetic materials, a new method known as the Stiffness Method was introduced in 2020. This method is described in Section 11 of the 2020 AASHTO LRFD Bridge Design Specifications.

Given this recent change in the American specification, the primary goal of this article is to conduct an analysis of the three methods available in AASHTO and compare the results obtained from real-scale MSE walls with the predicted values of T_{max}. This comparative study aims to provide insights into the accuracy and reliability of these methods in predicting the maximum reinforcement loads for various types of MSE wall systems, considering the specific characteristics of the reinforcement materials used, whether inextensible (e.g., steel) or extensible (e.g., geosynthetic).

2 Maximum reinforcement load Tmax

The Maximum Reinforcement Loads (Tmax) represent the force exerted on the MSE reinforcement at a specific depth. The value of Tmax depends on several factors, including vertical stress, soil strength, reinforcement spacing, reinforcement stiffness, and the type of facing used.

The calculation of the Maximum Reinforcement Loads for each layer of reinforcement employs different methods based on the type of reinforcement (these methods are detailed below): **Coherent Gravity Method** (inextensible materials), **Stiffness Method** (extensible materials), S**implified Method (**both steel and geosynthetic-reinforcement).

2.1 Coherent Gravity Method

In the Coherent Gravity Method, the reinforced wall mass is regarded as a rigid entity. To calculate the vertical stress at each level of reinforcement, an equivalent uniform pressure is computed. This pressure considers the impact of load eccentricity, which arises from the lateral earth pressure exerted at the back of the reinforced soil mass above the reinforcement level under consideration. This base pressure is applied across an effective width of the reinforced wall.

The Coherent Gravity Method is specifically intended for use with inextensible soil reinforcement systems, such as those employing steel. However, it should not be applied to walls constructed with cohesive backfill, which refers to soil possessing a plastic index greater than 6.

For steel-reinforced wall systems, the lateral earth pressure coefficient is determined as follows: It equals k_o at the point where the theoretical failure surface intersects the ground surface at or above the top of the wall. It transitions to k_a at a depth of 6 meters (20.0 feet) below that intersection point. Beyond this depth of 6 meters (20.0 feet), it remains constant at k_a, as depicted in Figure 1. See Allen et al. (2001) for additional information regarding the Coherent Gravity Method.

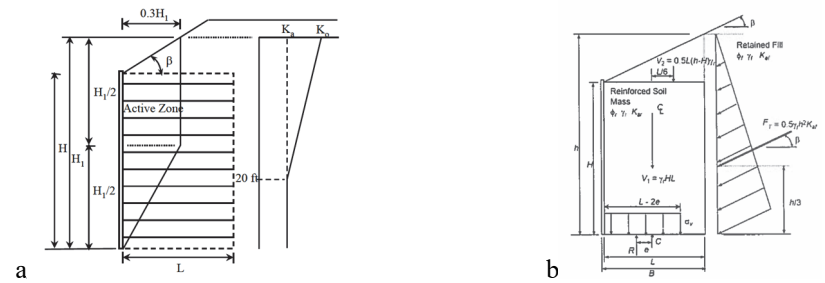

Fig. 1. Coherent Method analysis (a) Determination of Lateral Earth Pressure Coefficients and (b) forces and stress (AASHTO 2020)

The calculation of T_{max} using the Coherent Gravity Method is summarized in Eqs. 1 through 4:

$$T_{max} = S_v k_r \sigma_v \tag{1}$$

$$\sigma_v = \frac{V_1 + V_2 + F_T \sin\beta}{L - 2e} \tag{2}$$

$$e = \frac{F_T(\cos\beta)\, h/3 - F_T(\sin\beta)\, h/2 - V_2(L/6)}{V_1 + V_2 + F_T \sin\beta} \tag{3}$$

where: S_v is the tributary vertical thickness for reinforcement layer (m); k_r is the horizontal pressure coefficient of reinforced fill where k_r varies from K_0 to K_a as determined using Figure 1 -a (dim.); Z is the depth of reinforcement layer below wall top (m); γ_r is the unit weight of soil in wall reinforcement zone (kN/m^3); γ_f is the unit weight of soil backfill behind and above wall (kN/m^3); σ_v is the vertical stress at each reinforcement level (kPa); e is the eccentricity of the resultant force at the reinforcement location (m).

2.2 Simplified Method

In the Simplified Method, the load within the reinforcements is determined by multiplying the vertical earth pressure at the level of the reinforcement layer by a lateral earth pressure

coefficient that has been empirically adjusted (Figure 2). The lateral pressure obtained is then applied to the tributary layer thickness for the reinforcement to estimate the reinforcement load, T_{max}.

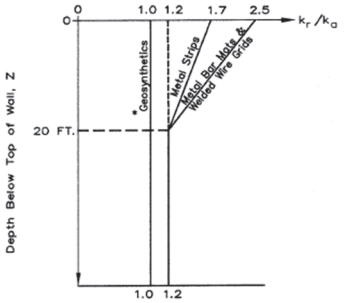

Fig. 2. Variation of the Coefficient of Lateral Stress ratio, Kr/ka (AASHTO 2020)

The vertical earth pressure at each level of reinforcement is calculated as the combination of the self-weight of the soil and any surcharge that may be present at that level. The reinforcement load, T_{max}, at each reinforcement level shall be determined as:

$$T_{max} = S_v k_r (\gamma_r Z + \gamma_f S) \tag{5}$$

where: S_v is the tributary vertical thickness for reinforcement layer (m); k_r is the horizontal pressure coefficient of reinforced fill determined using Figure 2 (dim.); Z is the depth of reinforcement layer below wall top (m); γ_r is the unit weight of soil in wall reinforcement zone (kN/m^3); γ_f is the unit weight of soil backfill behind and above wall (kN/m^3); S is the average soil surcharge thickness over reinforcement within 0.7H of the wall face (m).

2.3 Stiffness Method

The Stiffness Method is specifically intended for use with extensible soil reinforcement systems, such as geosynthetics like geotextiles, geogrids, and geostrips, as showed at AASHTO 2020, however Allen and Bathurst (2018) showed that this method can also be applied for steel. This method offers several advancements and advantages over prior methods. It addresses key parameters known to influence reinforcement loads, provides a more accurate prediction of T_{max}, and is adaptable to a broader range of soil types. It also handles facing batter more accurately and seamlessly covers all soil reinforcement types, including steel. Moreover, it allows for addressing service limits when assessing and designing for reinforcement strain and is calibrated according to the Load and Resistance Factor Design (LRFD) standards.

T_{max} shall be determined as follows using the Stiffness Method:

$$T_{max} = S_v \left[H\gamma_r D_{tmax} + \gamma_f \left(\frac{H_{ref}}{H} \right) S \right] k_{avh} \Phi \tag{6}$$

where: S_v is the tributary vertical thickness for reinforcement layer (m); H is the height of wall (m); H_{ref} is the reference wall height = 6m (m); γ_r is the unit weight of soil in wall reinforcement zone (kN/m^3); γ_f is the unit weight of soil backfill behind and above wall (kN/m^3); S is the average soil surcharge thickness over reinforcement ; D_{tmax} is the T_{max} distribution factor (dim.); k_{avh} is the active earth pressure coefficient for a wall with vertical face (dim.); Φ is the empirically determined influence factor that captures the effect that the soil reinforcement properties, soil cohesion, and wall geometry have on T_{max} (dim.).

D_{tmax} shall be determined as follows:

For $z < z_b$:
$$D_{tmax} = D_{tmax0} + \frac{z}{z_b}(1 - D_{tmax0}) \quad (7)$$

For $z \geq z_b$: $D_{tmax} = 1$

$$z_b = C_h(H)^{1.2} \quad (8)$$

$$\Phi = \Phi_g \Phi_{fs} \quad (9)$$

$$\Phi_g = 0.16\left(\frac{S_{global}}{P_a}\right)^{0.26} \quad (10)$$

$$S_{global} = \frac{J_{ave}}{(H/n)} = \frac{\sum_{i=1}^{n} J_i}{H} \quad (11)$$

where: Z is the depth of reinforcement layer below top of wall at wall face (m); Z_b is the depth below top of wall at wall face where D_{tmax} becomes equal to 1.0 (and below which D_{tmax} equals 1.0) (m); D_{tmax0} is the T_{max} distribution factor magnitude at top of wall at wall face, equal to 0.12 (dim.); C_h is the coefficient equal to 0.32 when H is in ft and 0.40 when H is in meters; Φ_g is the global stiffness factor (dim.); Φ_{fs} is the facing stiffness factor (dim.); S_{global} is the global reinforcement stiffness (kN/m); P_a is the atmospheric pressure at sea level (equals 101.325 kPa); J_{ave} is the average secant tensile stiffness of all n reinforcement layers (kN/m); J_i is the secant tensile stiffness of reinforcement layer i considering the horizontal spacing, i.e., the coverage ratio R_c, of the reinforcement (kN/m); n is the number of reinforcement layers in wall section (dim.)

2.4 Full-scale MSE walls

A comprehensive, long-term research program conducted at the Royal Military College of Canada (RMC) from 1998 to 2021 aimed to collect quantitative data on the behaviour of reinforced soil walls under controlled laboratory conditions. This involved the construction of over fifteen extensively monitored, 3.6-meter-high, full-scale reinforced soil walls. The instrumentation included strain gauges and extensometers affixed to reinforcement layers, connection load cells, horizontal and vertical toe load cells, earth pressure cells, and displacement measuring devices both at the wall face and the backfill surface.

The findings from these reinforced walls have been extensively documented in numerous articles, some of which are featured in publications such as Bathurst (2014), Bathurst et al. (2000, 2006, 2009). This study focused on examining four reinforced walls from the RMC full-scale program. Among these walls, four instrumented walls were chosen where the first two were reinforced using a polypropylene (PP) geogrid, the third with a PET geogrid, and the last one with a welded wire mesh. Notably, these walls had previously been assessed in comparison with the K-stiffness method as detailed in the article by Bathurst et al. (2009).

3 Results and discussion

Comparisons were made among the results obtained from four walls utilizing the three methodologies outlined in the latest AASHTO version (2020) as depicted in Figures 3 to 5. These methodologies were previously delineated in this paper, while the geometric specifications and soil properties for the four walls are detailed below.

The global reinforcement stiffness for each wall was as follows: Wall 1 – 477 kN/m², Wall 2 – 238 kN/m², Wall 5 - 153 kN/m², and Wall 6 - 5170 kN/m². All walls have the

same geometry specifications, including a height (H) of 3.6m, a target facing batter of ω=8° from the vertical, six layers of reinforcement each with a length of 2.2m, vertical spacing (Sv) of 0.6m, and concrete blocks for facing walls measuring 0.15m in height and 0.3m in width.

The backfill utilized uniformly graded sand (SP per USCS). The (secant) peak plane-strain friction angle was φ_{ps} = 44° (Hatami and Bathurst, 2005). Walls 1 and 2 were compacted using a vibrating-plate compactor, presenting a measured bulk unit weight during construction of γ=16.8 kN/m³. In contrast, Walls 5 and 6 (Wall 5 and Wall 6) were compacted with an electrically powered vibrating hammer, resulting in a measured bulk unit weight of γ=17.2 kN/m³. Further insights into the compaction effect were discussed in Bathurst et al. (2009).

Figure 3 presents the outcomes of Walls 1 and 2. Although these two walls shared identical design and reinforcement, every second longitudinal geogrid member was removed in Wall 2, leading to a material with half the stiffness and strength of the reinforcement in Wall 1. The measured results from Walls 1 and 2 exhibited similarities. The Coherent Gravity and Simplified methods yielded comparable analyses for both walls, as they do not account for reinforcement stiffness. However, the Stiffness Method showed variations between the walls due to its consideration of reinforcement stiffness.

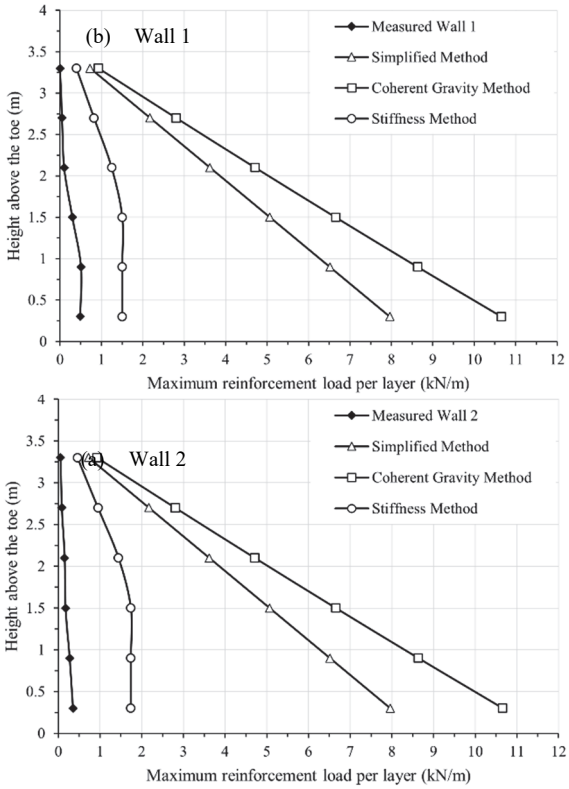

Fig. 3. Comparison between the predicted T_{max} method and (a) T_{max} measured at Wall 1 and (b) T_{max} measured at Wall 2 (half the stiffness and strength of the reinforcement in the Wall 1).

Figure 4 presents the measured results obtained from Wall 5, employing a PET geogrid as the reinforcement, which denotes a less rigid material. Meanwhile, Figure 5 portrays the outcomes from Wall 6 utilizing welded wire mesh reinforcement. Notably, in Figure 5, the upper section of the wall results exhibits strong agreement across all methods. However,

discrepancies become more pronounced in subsequent results, revealing an increasing disparity between anticipated values and those measured.

The collected data indicates that for walls reinforced with polymeric materials, the reinforcement loads demonstrate greater uniformity with depth. Additionally, the measured loads are notably lower than the values computed using the AASHTO (2020) methods. The discrepancy between the measured and predicted load values increases with the depth of the layer beneath the wall crest, particularly evident when employing the coherent gravity and simplified methods.

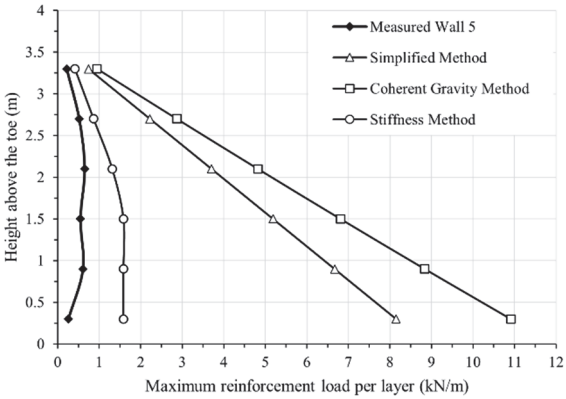

Fig. 4. Comparison between the predicted T_{max} method and T_{max} measured at Wall 5 (PET geogrid).

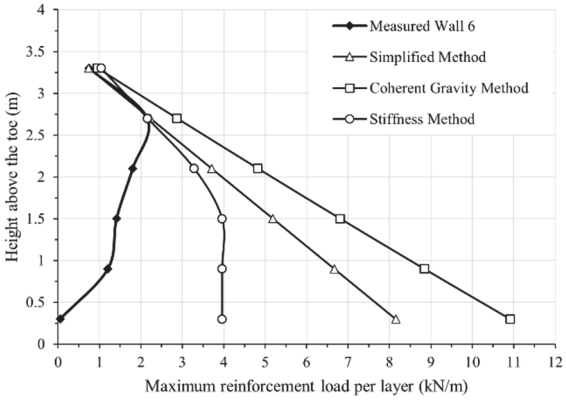

Fig. 5. Comparison between the predicted T_{max} method and T_{max} measured at Wall 6 (wire mesh).

4 Conclusions

This paper conducted a comparison among the three AASHTO (2020) methods used to predict the internal maximum tension on reinforcement, analyzing results obtained from four heavily instrumented full-scale walls, yielding valuable insights. The study revealed that all three AASHTO methods were conservative, consistently presenting values greater than those measured in the full-scale walls, affirming the safety in their application.

In cases of walls reinforced with geosynthetics (Wall 1, 2, and 5), the stiffness method exhibited higher accuracy, successfully capturing uniform reinforcement load distributions. Conversely, both the Coherent Gravity and Stiffness methods displayed significant discrepancies when compared to the measured values.

Regarding the welded wire mesh (WWM) wall, the computed reinforcement loads closely aligned across all methods in the upper portion of the wall, approaching values

similar to the Simplified and Stiffness methods. However, these methods showed a noticeable deviation from measured values in the lower section of the wall. Despite this, the predicted values remained consistently higher. The overprediction observed using the AASHTO method can be attributed to its inherent excessive conservatism.

The authors acknowledge the support of Coordenação de Aperfeiçoamento de Pessoal de Nível Superior - Brasil (CAPES) - Finance Code 001.

References

1. AASHTO. LRFD Bridge Design Specifications. American Association of State Highway and Transportation Officials (AASHTO), 9th Ed., Washington, D.C., USA (2020).
2. FHWA. Design and Construction of Mechanically Stabilized Earth Walls and Reinforced Soil Slopes, Vol. I. National Highway Institute Federal Highway Administration U.S. Dept. of Transportation, Washington, D.C., USA (FHWA-NHI-10-024) (2009).
3. CSA. Canadian Highway Bridge Design Code (CHBDC). CSA Standard S6-06. Canadian Standards Association (CSA), Toronto, Ontario, Canada, (2006).
4. NCMA. Design Manual for Segmental Retaining Walls (3rd ed.). Nat. Concrete Masonry Association, Herndon, VA, USA, (2009).
5. Allen, T.M., Christopher, B.R., Elias, V. and DiMaggio, J.D. Development of the Simplified Method for internal stability design of mechanically stabilized earth (MSE) walls. Report WA-RD 513.1, Washington State Department of Transporta-tion (WSDoT), Olympia, Wash., USA (2001).
6. Allen T.M. and Bathurst R.J. Application of the Simplified Stiffness Method to design of reinforced soil walls. Journal of Geotechnical and Geoenvironmental Engineering, 144(5): 04018024 (2018).
7. Bathurst, R.J. Challenges and recent progress in the analysis, design and modelling of geosynthetic reinforced soil walls, Giroud Lecture, CD Proceedings of the 10th International Geosynthetics Conference, Berlin, 21-25 September 2014, 38 p. (2014)
8. Bathurst, R.J., Walters, D., Vlachopoulos, N., Burgess, P. and Allen, T.M. Full scale testing of geosynthetic reinforced walls. Invited keynote paper, ASCE Special Publication No. 103, Advances in Transportation and Geoenvironmental Systems using Geosynthetics, Geo-Denver 2000, Denver, Colorado, pp. 201-217 (2000).
9. Bathurst, R.J., Vlachopoulos, N., Walters, D.L., Burgess, P.G. and Allen, T.M. The influence of facing rigidity on the performance of two geosynthetic reinforced soil retaining walls. Canadian Geotechnical Journal 43(12): 1225-1237 (2006).
10. Bathurst, R.J., Nernheim, A., Walters, D.L., Allen, T.M., Burgess, P. and Saunders, D. Influence of reinforcement stiff-ness and compaction on the performance of four geosynthetic reinforced soil walls. Geosynthetics International 16(1): 43-59, (2009).
11. Hatami, K. and Bathurst, R.J. Development and verification of a numerical model for the analysis of geosynthetic rein-forced soil segmental walls under working stress conditions. Canadian Geotechnical Journal 42(4): 1066-1085, (2005).